https://doi.org/10.5194/se-2020-136
Preprint. Discussion started: 16 September 2020

Solid Earth Discussions

Seismic evidences of the COVID-19 lockdown measures: Eastern Sicily case of study

Andrea Cannata[1,2], Flavio Cannavò[2], Giuseppe Di Grazia[2], Marco Aliotta[2], Carmelo Cassisi[2], Raphael S. M. De Plaen[3], Stefano Gresta[1], Thomas Lecocq[4], Placido Montalto[2], Mariangela Sciotto[2]

[1]Dipartimento di Scienze Biologiche, Geologiche e Ambientali, Università Degli Studi di Catania, Catania, Italy.
[2]Istituto Nazionale di Geofisica e Vulcanologia, Osservatorio Etneo, Catania, Italy.
[3]Centro de Geociencias, Universidad Nacional Autónoma de México, Campus Juriquilla, Querétaro, Mexico.
[4]Seismology-Gravimetry, Royal Observatory of Belgium, Avenue circulaire 3, 1180 Brussels, Belgium.

Correspondence to: Andrea Cannata (andrea.cannata@unict.it)

Abstract. During the COVID-19 pandemic, most countries worldwide put in place social interventions, consisting of restricting the mobility of citizens, aimed at slowing and mitigating the spread of the epidemic. In particular, Italy, as the first European country violently struck by the COVID-19 outbreak, applied a sequence of progressive restrictions to reduce both human mobility and human-to-human contacts from the end of February to mid-March 2020. Here, we analysed the seismic signatures of these lockdown measures in the densely populated Eastern Sicily, characterised by the presence of a permanent seismic network used for both seismic and volcanic monitoring. We specifically emphasize how the amount of the amplitude reduction of anthropogenic seismic noise (reaching ~50-60%), its temporal pattern and spectral content are strongly station-dependent. As for the latter, we exhibited that on average the frequencies above 10 Hz are the most influenced by the anthropogenic seismic noise. Finally, we found an impressive similarity between the temporal patterns of anthropogenic seismic noise and human mobility, as quantified by the mobile phone-derived data shared by Google, Facebook and Apple. These results further confirm how seismic data, routinely acquired worldwide for seismic and volcanic surveillance, can be used to monitor human mobility too.

1. Introduction

During the end of 2019, several cases of pneumonia, due to the novel coronavirus SARS-CoV-2, were identified in the city of Wuhan, China (Wang et al., 2020a). The related disease, called COVID-19, then rapidly spread from China to other areas, as a pandemic wave (as declared by the World Health Organisation, WHO, in March 2020) currently affecting 216 countries with almost 14,300,000 confirmed cases (at the time of writing 21 July 2020; WHO, 2020). COVID-19 is considered the most severe global health crisis of our time and the greatest challenge human beings have faced since World War Two (WHO, 2020).

https://doi.org/10.5194/se-2020-136
Preprint. Discussion started: 16 September 2020

While huge efforts are being made to find pharmacological cures to heal the sick and to stop the spread of the disease (e.g. Cannata et al., 2020a; Graham, 2020; Wang et al., 2020b), most of the countries worldwide put in place social interventions, consisting of restricting the mobility of citizens, aimed at slowing and mitigating the epidemic (Pepe et al., 2020). Italy was the first country in Europe to be violently struck by the COVID-19 pandemic wave at the end of February – onset of March 2020. Hence, Italy was also the first European country to apply a sequence of progressive restrictions to reduce both human mobility and human-to-human contacts. Restrictions were first implemented on 23 February 2020 in some regions of Northern Italy (Lombardy, Emilia-Romagna, Veneto, Friuli-Venezia Giulia, Piedmont, and Autonomous Province of Trento). Between 8-11 March, the entire country was put under lockdown (Gatto et al., 2020).

To provide information about the effectiveness of the quarantine measures during COVID-19 emergency, Apple, Facebook and Google made available mobility data, mostly based on mobile phone locations, for almost every country in the world (Apple, 2020; Facebook, 2020; Google, 2020). At the same time, different studies showed the effectiveness of seismic noise monitoring as a tool to quantify human activity and its changes over time (Dias et al., 2020; Hong et al., 2020; Lindsey et al., 2020; Lecocq et al., 2020). Indeed, the Earth is continuously vibrating due to a wide spectrum of elastic energy sources including tectonic forces (Stein and Wysession, 2003), volcanic processes (Chouet and Matoza, 2013), ocean (Cannata et al., 2020b) and human (Diaz et al., 2017) activity. As for the latter, it typically generates a high-frequency continuous signal (> 1 Hz), called anthropogenic or cultural seismic noise, associated with phenomena such as traffic, construction, industrial operations and mining (Diaz et al, 2017; Hong et al., 2020). Recent papers identified clear seismic signatures of the lockdown measures applied by different countries (Lindsey et al., 2020; Lecocq et al., 2020; Poli et al., 2020; Xiao et al., 2020). For instance, Lindsey et al. (2020) showed a 50% decrease in vehicle count in Palo Alto area (California) immediately following the lockdown order by using fiber-optic distributed acoustic sensing connected to a telecommunication cable. Lecocq et al. (2020) performed a global-scale analysis of anthropogenic seismic noise using hundreds of seismometers located around the world, which evidenced how the 2020 lockdown period has produced the longest and most dramatic global anthropogenic seismic noise reduction on record.

In this work, we analyse the seismic signatures of the lockdown measures in the highly populated Eastern Sicily (Italy), which benefits from the presence of a dense permanent seismic network used for both seismic and volcanic monitoring. We investigate the decrease in the anthropogenic seismic noise amplitude, characterise its spectral content, and compare the observed changes with mobility data. Finally, we highlight the positive impact of such a noise level decrease on the capability to automatically detect and analyse earthquake signals.

https://doi.org/10.5194/se-2020-136
Preprint. Discussion started: 16 September 2020

2. Materials and methods

2.1 Data

The seismic data was recorded by 18 stations, located on the Eastern part of Sicily and belonging to the seismic permanent network, run by Istituto Nazionale di Geofisica e Vulcanologia, Osservatorio Etneo (INGV-OE) (Figures 1 and A1). These stations, selected both for the good data continuity and the even spatial distribution on the investigated area, are equipped with broadband (40 s cutoff period), 3-component Trillium Nanometrics™ seismometers, acquiring at a sampling rate of 100 Hz. The analysed time interval was 1 November 2019 – 23 May 2020.

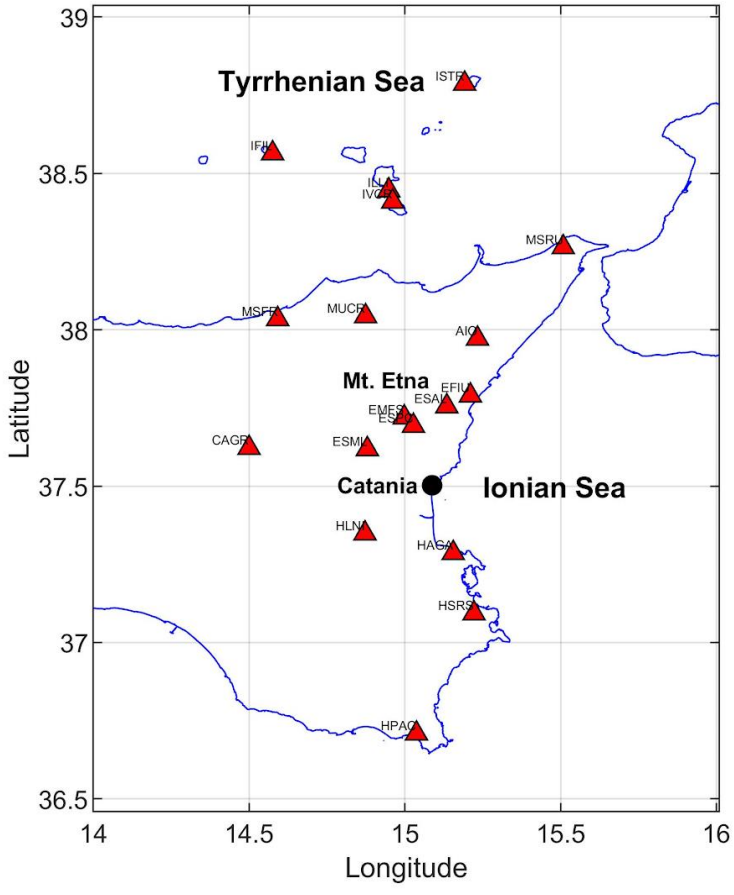

Figure 1. Map of the Eastern Sicily with the location of the seismic stations (red triangles) used in this work.

https://doi.org/10.5194/se-2020-136
Preprint. Discussion started: 16 September 2020

2.2 Spectral and amplitude analysis

75 Both spectral and amplitude analyses were carried out to characterise the temporal variations of the seismic noise features. As for the former, the daily spectra of the vertical component of the seismic signal were calculated by using Welch's method (Welch, 1967) with windows of 81.92 seconds. Finally, all the daily spectra were gathered and visualized as spectrograms, with time on the x-axis, frequency on the y-axis, and power spectral density (PSD) indicated by a color scale (Figure 2).

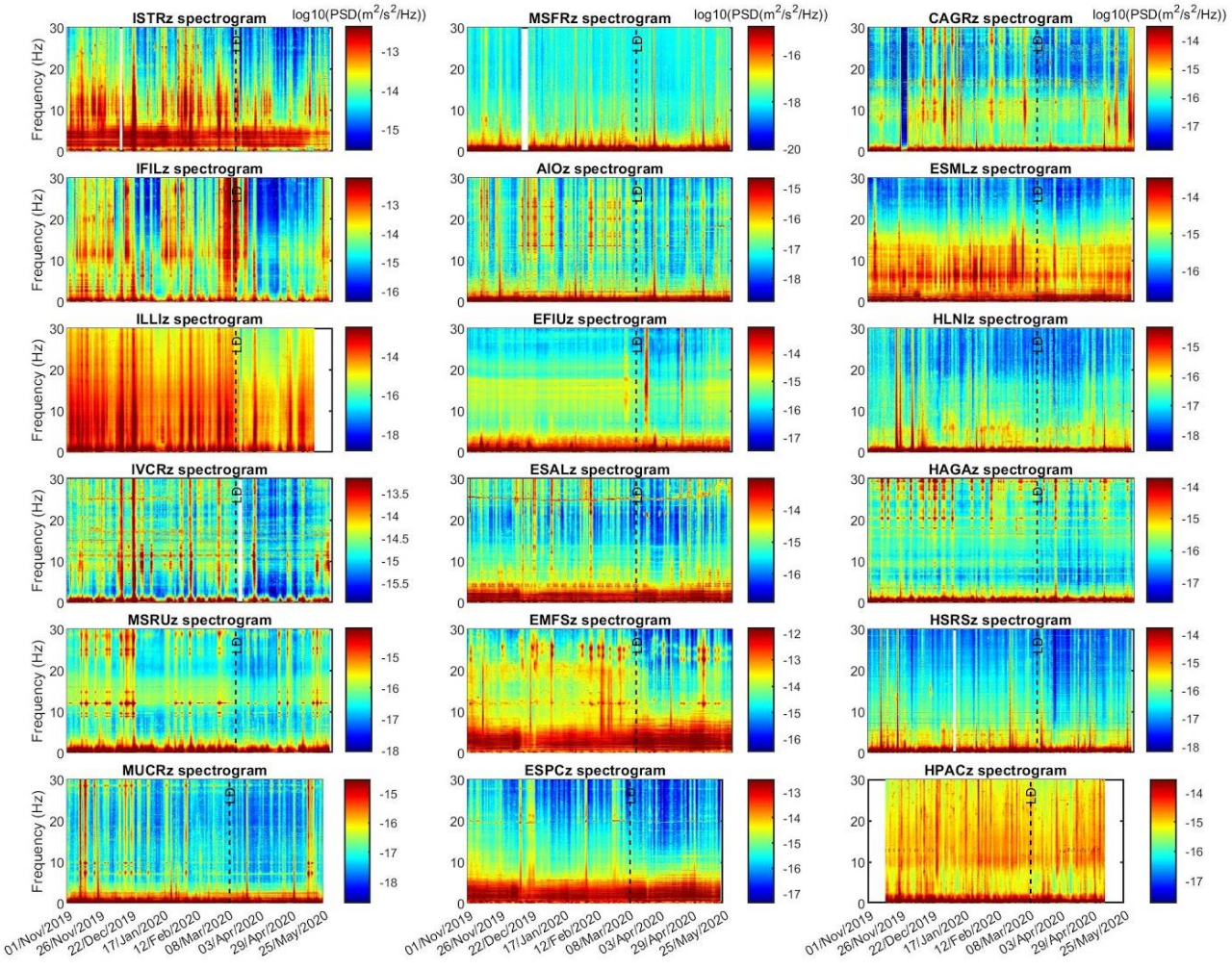

https://doi.org/10.5194/se-2020-136
Preprint. Discussion started: 16 September 2020

Figure 2. Spectrograms of the vertical component of the seismic signals. The vertical dashed line and the label "LD" indicate the time when the national lockdown measures were implemented in Italy (11 March 2020).

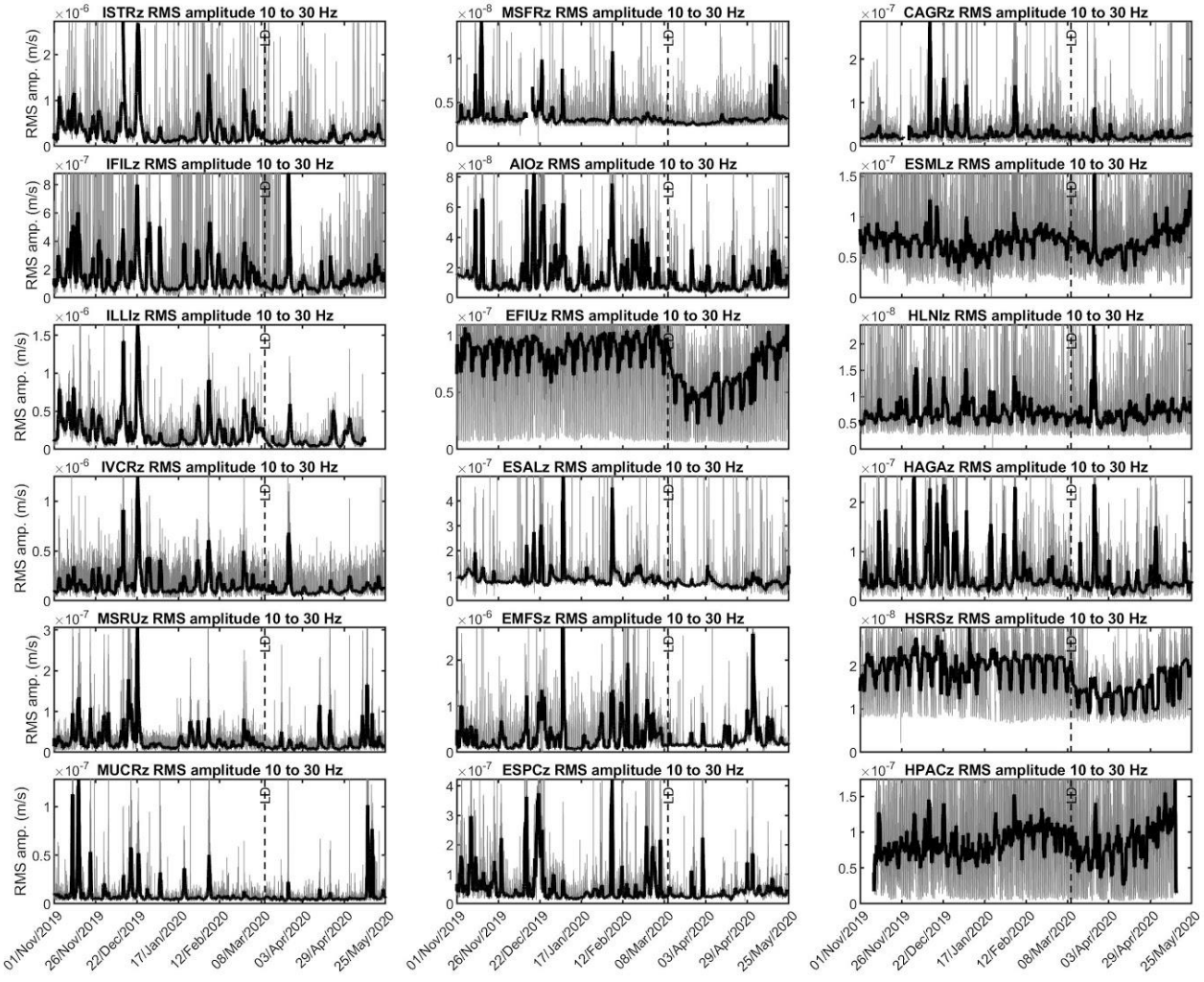

Figure 3. RMS amplitude time series of the vertical component of the seismic signals, filtered in the band 10-30 Hz (grey line) and corresponding moving median computed on 1-day-long sliding windows (thick black line). The vertical dashed line and the label "LD" indicate the time when the national lockdown measures were implemented in Italy (11 March 2020).

Concerning the amplitude analysis, the time series of the root mean square (RMS) amplitude of the seismic signal, filtered in the band 10-30 Hz, were obtained on 15-minute-long sliding windows (Figure 3). To visually show the general temporal pattern of the seismic noise amplitude in Eastern Sicily, the RMS amplitude time series were averaged on 3-day-long time

https://doi.org/10.5194/se-2020-136
Preprint. Discussion started: 16 September 2020

sliding windows, normalised, gathered and represented by a colored checkerboard plot (Figure 4). To make the changes of the noise background level as clear as possible in the checkerboard plot, the normalization was performed by: i) setting all the values greater than the 90th percentile, equal to the 90th percentile, ii) subtracting the minimum value, and iii) dividing by the maximum value. In addition, the percentage change in seismic RMS amplitude in the band 10-30 Hz in the period 11 March - 11 April 2020 was calculated by using the RMS amplitude during 20 January - 20 February 2020 as baseline (Figure 5).

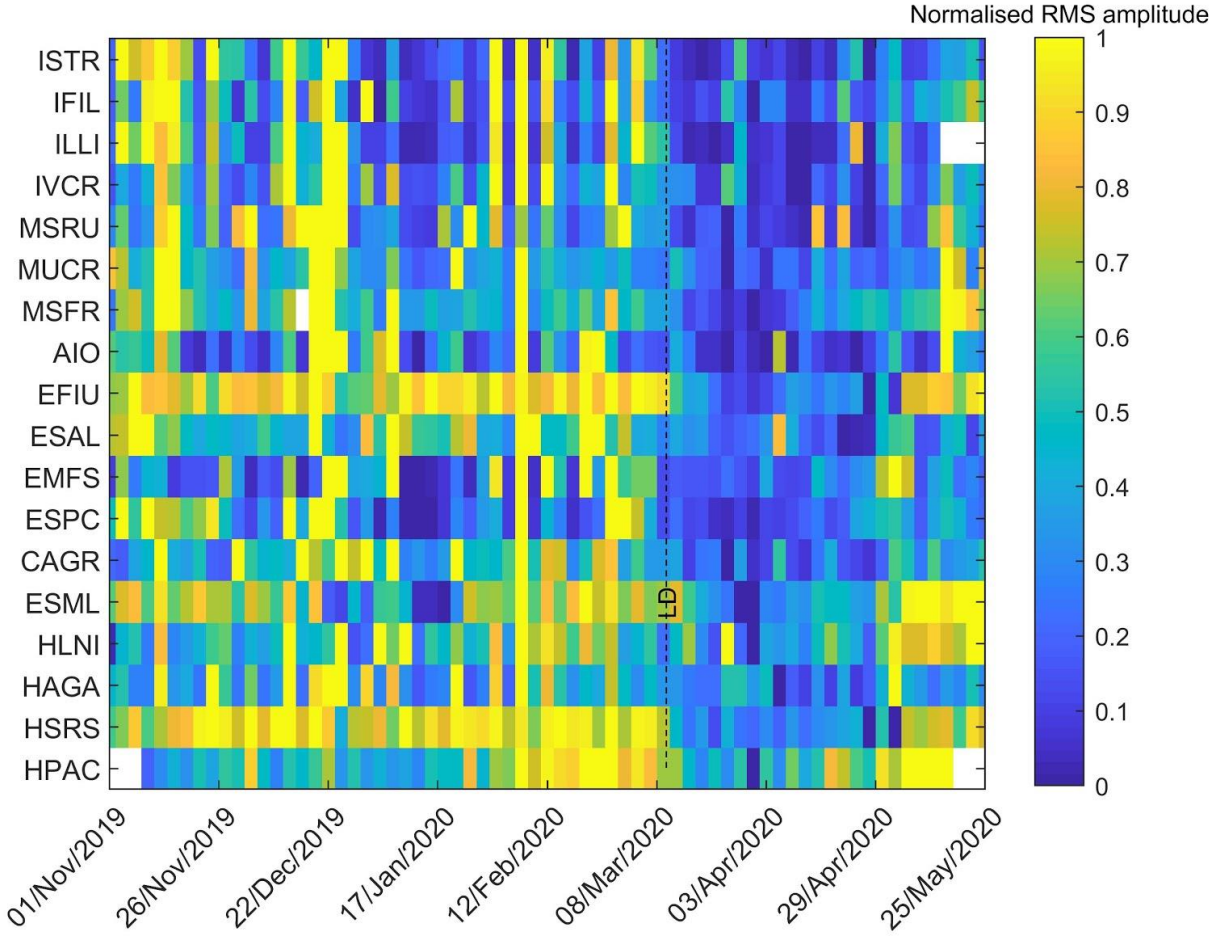

Figure 4. Temporal changes of the normalised seismic RMS amplitude at 18 seismic stations sorted by decreasing latitude (see labels close to the left y-axis). Data gaps are coloured white. The vertical dashed line and the label "LD" indicate the time when the national lockdown measures were implemented in Italy (11 March 2020).

https://doi.org/10.5194/se-2020-136
Preprint. Discussion started: 16 September 2020

Solid Earth
Discussions
Open Access
EGU

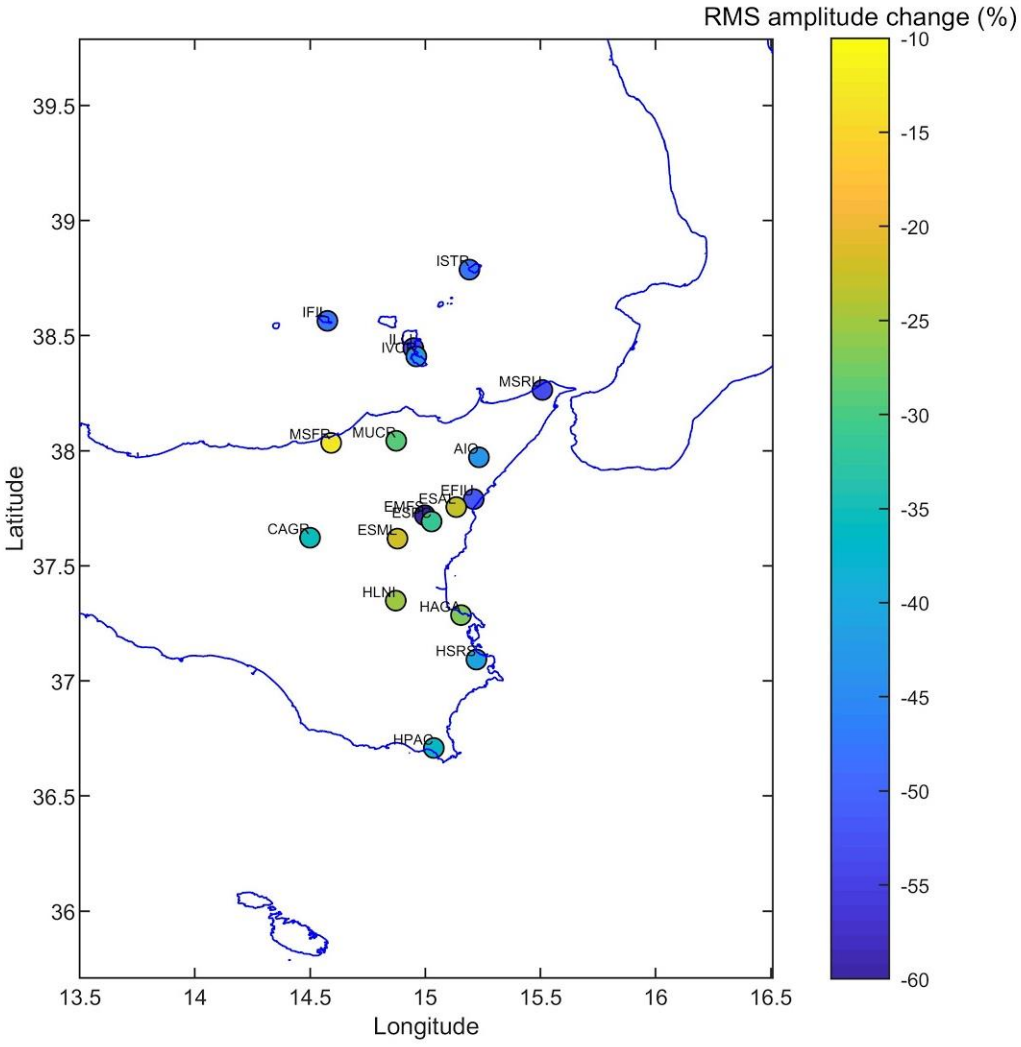

Figure 5. Percent change of seismic RMS amplitude in the band 10-30 Hz during the period 11 March - 11 April 2020 (right after the lockdown measures entered in force) with respect to the interval 20 January - 20 February 2020.

105 Finally, to highlight the frequency band showing the most evident amplitude changes due to the lockdown, two 20-day-long time windows, extracted before (1-20 February) and during (11 March – 1 April) the lockdown, were considered. Two average spectra, representing the seismic spectral content before and during the lockdown, were computed on the two windows, and, successively, a ratio between them was calculated (Figures 6 and 7). All the ratios were stacked and the result is shown in Figure 8.

https://doi.org/10.5194/se-2020-136
Preprint. Discussion started: 16 September 2020

Solid Earth
Discussions
Open Access
EGU

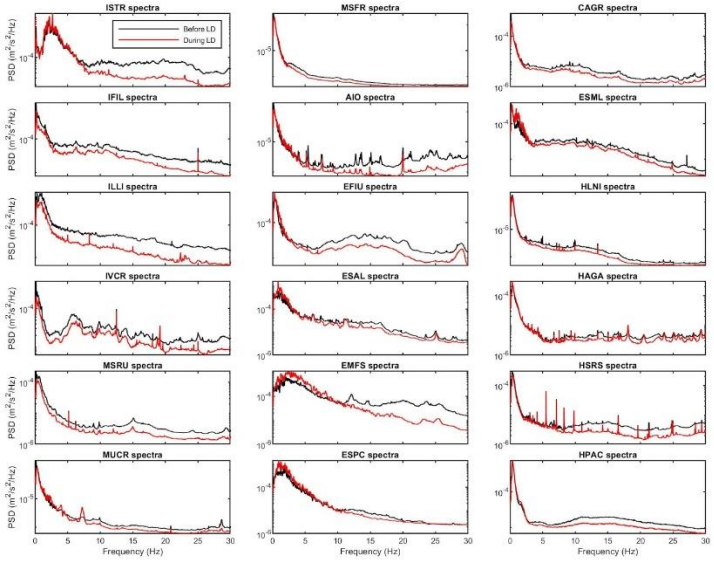

Figure 6. (a) Spectra of the vertical component of the seismic signals recorded during two 20-day-long time windows, extracted before (black line; 1-20 February) and during (red line; 11 March – 1 April) the lockdown.

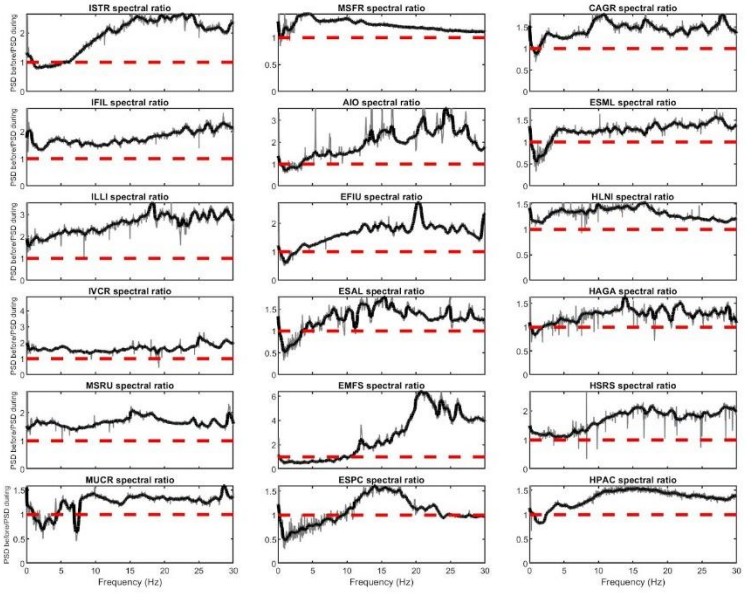

Figure 7. Ratio between the spectra of the vertical component of the seismic signals recorded during two 20-day-long time windows, extracted before (1-20 February) and during (11 March – 1 April) the lockdown (see Figure 6). The red horizontal dashed lines indicate ratio values equal to 1.

https://doi.org/10.5194/se-2020-136
Preprint. Discussion started: 16 September 2020

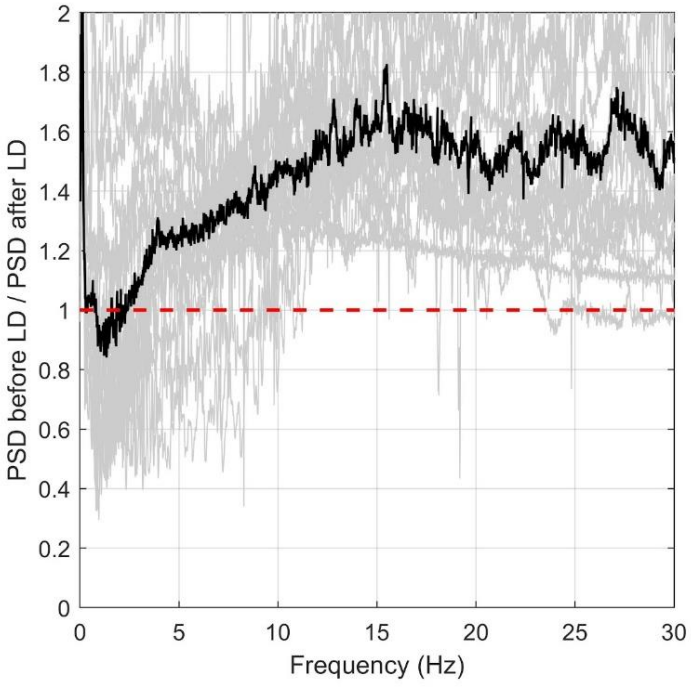

Figure 8. Ratios between the spectra computed before and during the lockdown (grey lines; see Figure 7) and the corresponding stacked ratio (black line). The red horizontal dashed line indicates a ratio value equal to 1.

2.3 Comparison with mobility data

Google, Apple and Facebook made human mobility data available for almost every country worldwide as support for public health policy during the COVID-19 crisis. For our study area, Google and Facebook provided aggregated data for the Sicily region, Apple shared data for Catania City, which is the main city in Eastern Sicily (Figure 1). The Google community mobility corresponds to the percentage of change relative to a baseline defined as the median value of the corresponding day of the week, during the period 3 January – 6 February 2020. The data are structured in categories to group some of the places with similar characteristics: grocery stores and pharmacy, parks, transit stations, retail and recreation places, residences and workplaces (Google, 2020). Apple shared information about the percent change of public's walking and driving compared with the baseline value from the 13 January (Apple, 2020). Finally, Facebook provided data regarding the human movement percent changes measured throughout March, April, and May 2020 relative to a baseline value in February (Facebook, 2020).

To understand how much the seismic noise could reflect the society mobility level, a correlation analysis was performed between the time series of the seismic RMS amplitude and the corresponding above mentioned community mobility data. In place of using the more common Pearson correlation coefficient, we made use of the Spearman correlation coefficient, allowing

https://doi.org/10.5194/se-2020-136
Preprint. Discussion started: 16 September 2020

to compare series which do not have a normal distribution, as well as to explore nonlinear relationships (e.g. Craig et al., 2016; Cannata et al., 2019). Figure 9 shows the Spearman correlation coefficient computed between seismic RMS amplitude in the 10-30 Hz range at the different stations and the community mobility datasets provided by Google, Apple and Facebook. An example of comparison between the time series of the RMS amplitude at EFIU station and the changes of mobility observed by Google is shown in Figure A2. To verify if the obtained Spearman correlation coefficients are significantly different from zero or not (null hypothesis), the t-test was performed and the p-value (probability value) was calculated (Figure A3). p-values lower than the significance level of 0.05 were considered sufficient to reject the null hypothesis.

Besides, to identify the frequencies that better correlate with the human mobility data, we performed the described correlation analysis for all the time series of seismic RMS amplitudes filtered in narrow bands (bandwidth = 1Hz, 4th order Butterworth filter; Lyons, 2004) around the integer frequencies between 1 and 30 Hz. Then, we considered the mean values of the Spearman correlation coefficient computed for all the stations (Figure 10).

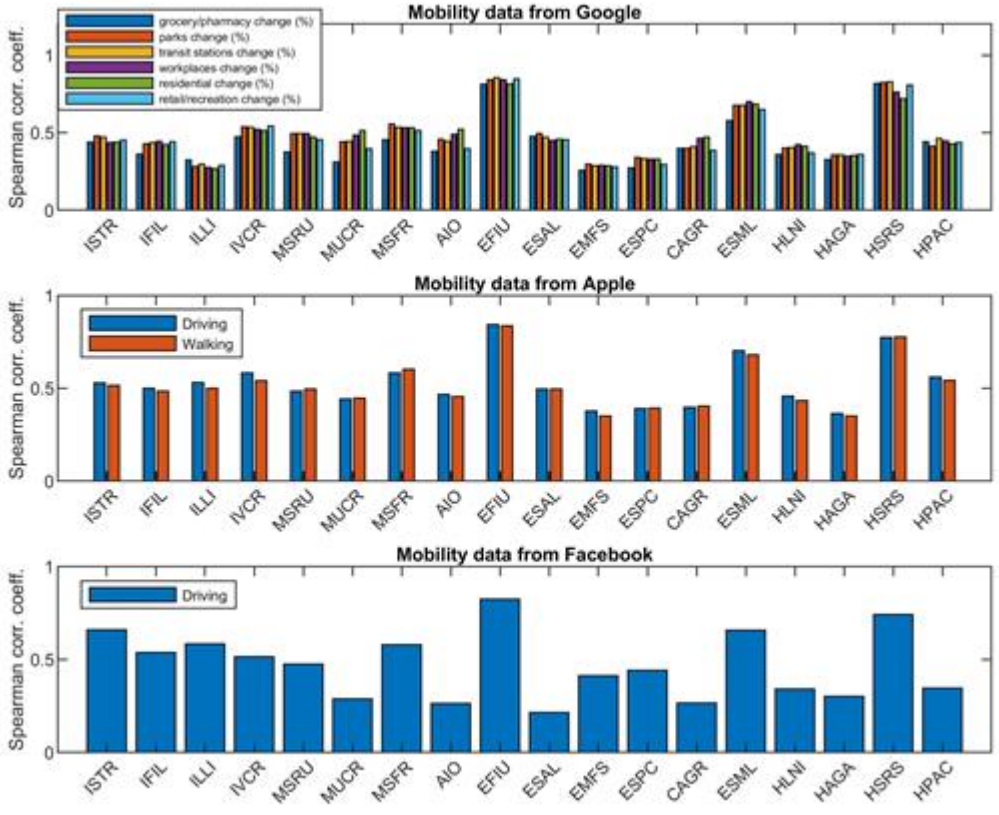

Figure 9. Spearman correlation coefficient calculated between seismic RMS amplitude at the different stations and the mobility parameters, as provided by Google, Apple and Facebook. The Spearman correlation coefficient obtained for the residential change (see top plot) was multiplied by -1 to make it positive.

https://doi.org/10.5194/se-2020-136
Preprint. Discussion started: 16 September 2020

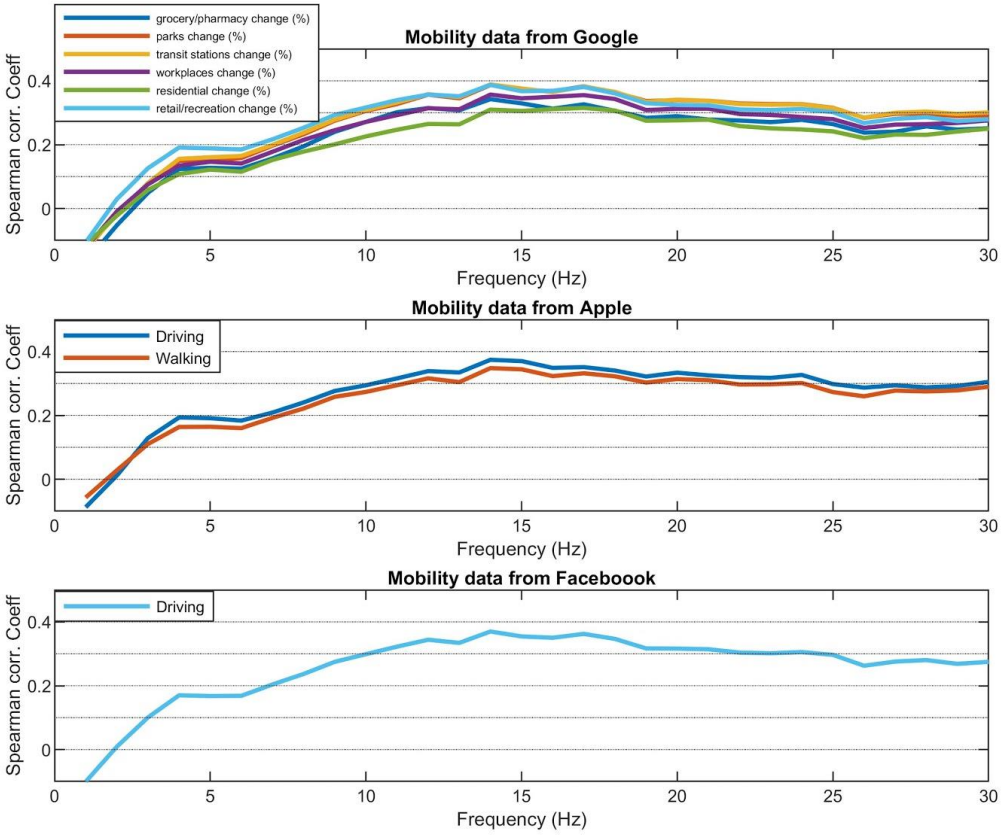

Figure 10. Spearman correlation coefficient, calculated between seismic RMS amplitude at the different stations and the mobility parameters, as a function of the frequency band of the seismic noise. The Spearman correlation coefficient obtained for the residential change (top plot) was multiplied by -1 to make it positive.

2.4 Effects on earthquake detection capability

The impact of the reduction of anthropogenic seismic noise during the lockdown period on the detectability of the earthquakes was analysed, by using the catalogue of the earthquakes automatically detected for the INGV-OE control room. The system, routinely applied at INGV-OE to monitor the mostly local seismicity in Eastern Sicily, is called *Kataloc* and uses the STA/LTA algorithm (short time average / long time average; Trnkoczy, 2012) to automatically pick the P seismic phases. The ability for this technique to detect amplitude transients in the real-time streaming of seismic data closely depends on the signal to noise ratio (e.g. Trnkoczy, 2012). The reduction of seismic noise during the lockdown period therefore motivated the analysis of its influence on the performances of this system.

https://doi.org/10.5194/se-2020-136
Preprint. Discussion started: 16 September 2020

We emphasized this influence by plotting the number of automatically detected P seismic phases per earthquake versus the earthquake magnitude before the lockdown (from 1 November 2019 to 10 March 2020) and during the lockdown period (from 11 March to 15 May 2020). We then performed linear regressions on the two sets of data, made up of 287 and 119 earthquakes, respectively (Figure 11a). Finally, since the number of detected seismic phases is strongly affected by the number of properly working seismic stations, we repeated the same analysis by using a number of detected P phases corrected according to the operating state of the seismic network. The correction was performed by dividing the number of phases by the fraction of seismic data acquired by the network during the day when the earthquake took place, with respect to the data which would have been recorded in case of full operating state of the network (Figure 11b).

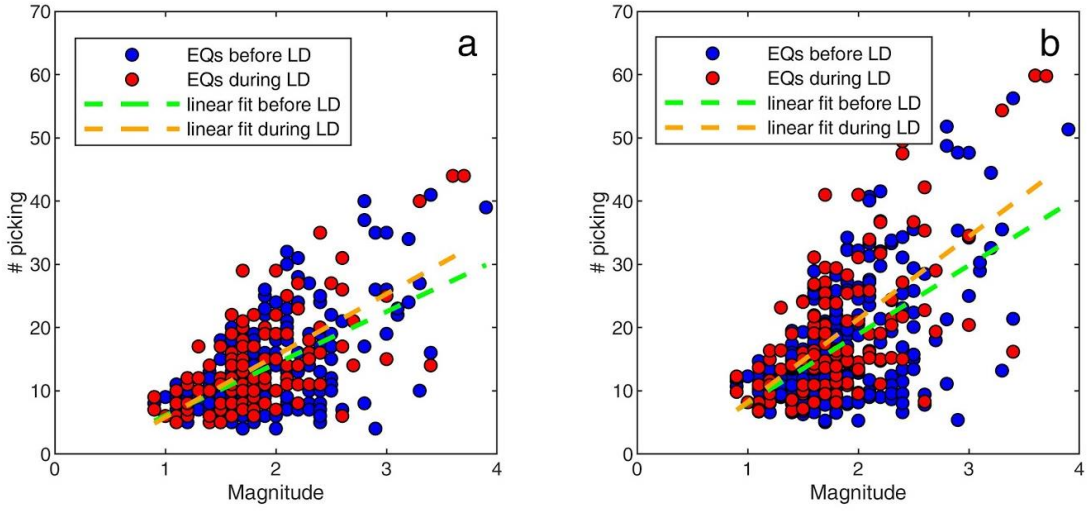

Figure 11. (a) Crossplot showing the magnitude of the earthquakes versus the number of automatic detections of P seismic phases during 1 November 2019 - 10 March 2020 (blue dots) and during 11 March - 15 May 2020 (red dots), and the corresponding fits to linear models (dashed green and orange lines, respectively). (b) Same as (a) with the number of automatic detections of P seismic phases corrected according to the operating state of the seismic network.

3. Results and discussion

The seismic data collected by 18 stations located in Eastern Sicily was analysed. A general reduction in the amplitude of seismic noise at all the stations is observed following the enforcement of lockdown measures (on 11 March 2020; Figures 2-5). However, the amount of reduction, as well as the pattern of the investigated seismic RMS amplitude time series varies significantly in function of the station considered. For instance, the stations located close to towns and infrastructures such as busy roads, highways and industrial plants (EFIU, ESML, HSRS, HPAC), show the typical temporal pattern of the

https://doi.org/10.5194/se-2020-136
Preprint. Discussion started: 16 September 2020

anthropogenic seismic noise with minima during the weekends and the night-time, and maxima during the weekdays and the day-time (Figure A4; Lecocq et al., 2020; Xiao et al., 2020). Focusing on the frequency band 10-30 Hz, the amplitude noise reduction due to the lockdown measures reaches ~50% at EFIU station (Figure 5), which also shows a slight amplitude decrease (~10%) during the Christmas - New Year holidays. This station is close to towns, as well as to a busy highway called A18 (Figure A1). Other stations show less regular patterns with clear peaks interspersed throughout the time series, whose origin depends also in this case on the station considered. In the stations located in the Aeolian Islands (ISTR, ILLI, IVCR, IFIL), the peaks are closely related to the ships rather than to road traffic or industrial activities (Figure A1 and A5). The amplitude and rate of occurrence of those peaks also clearly decreased right after the implementation of the lockdown measures. Overall, the reduction in seismic noise in the band 10-30 Hz in the Aeolian Islands ranges between ~40% - 50% (Figure 5). At stations EMFS, ESPC, located on the flanks of Mt. Etna, the anthropogenic seismic noise is mostly related to tourists' excursions, as both stations are located close to country roads used to bring tourists to the top of the volcano (Figure A1). These excursions were suspended on 9 March following the COVID-19 outbreak, leading to a decrease in the seismic noise in the band 10-30 Hz of 30% and 60% for ESPC and EMFS, respectively (Figure 5). Some notable increases in seismic amplitudes, visible in more than one stations at the same time, are not caused by human activities but rather due to bad weather conditions. For instance, the amplitude increase on 25-26 March, visible at almost all the stations (Figures 2 and 3), was associated with bad weather conditions, which affected the whole Southern Italy. The amplitude of the anthropogenic seismic noise interestingly increased again at the end of April - beginning of May, many days before the introduction of the Presidential Decree, partially releasing the lockdown measures, issued on 18 May 2020.

As for the frequency content analysis, the spectral ratios show that the band characterised by anthropogenic seismic noise is strongly station-dependent (Figure 7). Indeed, the frequency with the maximum ratio value, coinciding with the frequency most affected by the anthropogenic noise, ranges from a few Hz (i.e. MSFR) to 20 Hz or even more (i.e. EFIU, ESML). Besides, the maximum ratio value, which indicates the amount of anthropogenic noise affecting the station, shows a fairly wide variability, from 1.5 (i.e. ESPC, HPAC) to 6 (EMFS). It is also noteworthy that some stations show a ratio lower than 1 at low frequencies (a few Hz), indicating that the seismic amplitude was higher during the lockdown than before. The stations on or around Mt. Etna (ESPC, ESAL, EFIU, AIO, EMFS, ESML), as well as the station on Stromboli island (ISTR), exhibit this behaviour due to the increase of volcanic tremor amplitude in both volcanoes during the second analysed time window (11 March – 1 April) with respect to the first one (1-20 February). Indeed, Mt. Etna and Stromboli volcanoes are characterised by continuous volcanic tremor, with energy mainly radiated in the band ~0.5-5.5 Hz (e.g. Cannata et al., 2010; Falsaperla et al., 1998). In addition, the variability of the spectral ratio values below 1 Hz is not related to temporal changes in anthropogenic noise but rather to the variations in the amplitude of microseism, the most continuous and ubiquitous seismic signal on Earth, generated by ocean wave energy coupling with the Earth's ground (e.g. Longuet-Higgins 1950; Hasselmann, 1963; Ardhuin et al., 2015). Finally, the spectral ratio derived from stacking the spectral ratio plots of all the considered stations clearly

https://doi.org/10.5194/se-2020-136
Preprint. Discussion started: 16 September 2020

exhibits that the frequency band most affected by the anthropogenic seismic noise (that is, the one showing the highest ratio values) is above 10 Hz (Figure 8).

Concerning the comparison between the time series of seismic noise and human mobility, p-values lower than 0.05 were obtained in all the cases but the comparison between ESAL seismic noise and mobility data from Facebook (Figure A3). This suggests how the obtained Spearman correlation coefficients are significantly different from zero, confirming that seismic data contain plenty of information about human mobility. Seismic noise amplitude and all the different categories of community mobility are positively correlated, suggesting that seismic noise amplitude increases with increasing human mobility, with the exception of the residential visit changes provided by Google (Figure 9). Indeed, this category quantifies the change in duration of time spent at places of residence, which, unlike the other categories, increased during the lockdown period. In addition, the similarity between seismic noise and human mobility patterns displays a clear station dependence. Stations EFIU, ESML, HSRS, and HPAC display a typical temporal pattern of the anthropogenic seismic noise with minima during the weekends and maxima during the weekdays, which translated to the highest correlation coefficients. The similarity between seismic noise and human mobility patterns is remarkably high at station EFIU which exhibits correlation coefficients higher than 0.8 (Figure A2). The seismic noise frequencies better correlated with human mobility data turned out to be above 10 Hz (maximum values are reached in the band 11 - 18 Hz; Figure 10). This result, in line with the information obtained by computing the ratios between the seismic spectra before and during the lockdown (Figure 8), shows how the seismic frequency band most affected by the human activities is above 10 Hz.

Finally, during the period 11 March - 15 May 2020 *Kataloc* system reported a higher number of detected P seismic phases per earthquake, magnitude being equal (Figure 11). This demonstrates that the decrease in anthropogenic seismic noise amplitude during the lockdown period had a direct effect on the catalogue of earthquakes collected during that interval.

4. Conclusions

The amplitude reduction of the anthropogenic seismic noise, due to the lockdown measures restricting the mobility of citizens during the COVID-19 pandemic, gave the opportunity to investigate in detail the characteristics of such an anthropogenic signal in Eastern Sicily.

The amount of amplitude reduction of anthropogenic seismic noise, its temporal pattern and spectral content proved to be strongly station-dependent. As for the former, we found decreases of 30-60% in most of the considered stations, located close to towns and busy highways, as well as on the flanks of Mt. Etna where country roads are used to bring tourists on the top of the volcano, or even in the Aeolian Islands following to ship traffic reduction. Regarding the temporal patterns of seismic noise amplitude, the stations installed close to towns or infrastructures (like busy roads, highways and industrial plants) showed the typical pattern of the anthropogenic seismic noise with minima during the weekends and the night-time, and maxima during

https://doi.org/10.5194/se-2020-136
Preprint. Discussion started: 16 September 2020

the weekdays and the day-time. Other stations show less regular patterns with clear peaks interspersed throughout the time series. Concerning the spectral content, the frequency band most affected by anthropogenic seismic noise ranges from a few Hz to more than 20 Hz, depending on the station. On average, the frequencies above 10 Hz are the most influenced by anthropogenic seismic noise. Such a reduction in anthropogenic seismic noise amplitude was also reflected in the enhanced capability to automatically detect earthquake seismic phases.

Finally, we found that human mobility influenced the seismic noise mostly in frequencies above 10 Hz with remarkably high correlations between them observed at some stations. These results further confirm how seismic data, routinely acquired worldwide mainly for seismic and volcanic surveillance, can also be used to monitor human mobility, especially during emergency periods such as the COVID-19 pandemic. As highlighted by Lindsey et al. (2020), seismic data also present the advantages over mobile phone-derived information of being natively anonymous and not affected by biases due to data sampling according to socio-economic class, age and region.

Data availability

The data that support the findings of this study are available on request from the corresponding author.

Author contributions

A.C., F.C. and T. L. designed the study. All the Authors analysed the seismic data. A.C., F.C., R.D.P., G.D.G. wrote the paper. All the Authors interpreted the results and revised the article.

Competing interests

The authors declare that they have no conflict of interest.

Acknowledgements

We are indebted to the technicians of the INGV-OE for enabling the acquisition of seismic data. We also sincerely acknowledge all the essential workers who, placing themselves at risk, took care of the sicks, assisted the communities, and served in any way during the COVID-19 pandemic. This work was funded by CHANCE project, II Edition, Università degli Studi di Catania.

https://doi.org/10.5194/se-2020-136
Preprint. Discussion started: 16 September 2020

References

Apple: Mobility Trends Reports. Available at: https://www.apple.com/covid19/mobility, 2020 (accessed: 05 June 2020).

Ardhuin, F., Gualtieri, L., and Stutzmann, E.: How ocean waves rock the Earth: Two mechanisms explain microseisms with periods 3 to 300 s, Geophys. Res. Lett., 42, 765–772, https://doi.org/10.1002/2014GL062782, 2015.

Cannata, A., Di Grazia, G., Montalto, P., Ferrari, F., Nunnari, G., Patanè, D., and Privitera, E.: New insights into banded tremor from the 2008–2009 Mount Etna eruption, J. Geophys. Res., 115, 1–22, 2010.

Cannata, A., Cannavò, F., Moschella, S., Gresta, S., and Spina, L.: Exploring the link between microseism and sea ice in Antarctica by using machine learning, Sci. Rep., 9, 13050, 2019.

Cannata, F., Chiarito, M., Reimers, B., Azzolini, E., Ferrante, G., My, I., Viggiani, G., Panico, C., Regazzoli, D., Ciccarelli, M., Voza, A., Aghemo, A., Li, H., Wang, Y., Condorelli, G., and Stefanini, G.G.: Continuation versus discontinuation of ACE inhibitors or angiotensin II receptor blockers in COVID-19: effects on blood pressure control and mortality, European Heart Journal - Cardiovascular Pharmacotherapy, pvaa056, https://doi.org/10.1093/ehjcvp/pvaa056, 2020a.

Cannata, A., Cannavò, F., Moschella, S., Di Grazia, G., Nardone, G., Orasi, A., Picone, M., Ferla, M., and Gresta, S.: Unravelling the Relationship Between Microseisms and Spatial Distribution of Sea Wave Height by Statistical and Machine Learning Approaches, Remote Sensing, 12(5), 761, https://doi.org/10.3390/rs12050761, 2020b.

Chouet, B. A., and Matoza, R. S.: A multi-decadal view of seismic methods for detecting precursors of magma movement and eruption, J. Volcanol. Geotherm. Res., 252, 108– 175, doi:10.1016/j.jvolgeores.2012.11.013, 2013.

Craig, D., Bean, C., Lokmer, I., and Mollhoff, M.: Correlation of Wavefield-Separated Ocean-Generated Microseisms with North Atlantic Source Regions, Bulletin of the Seismological Society of America, 106, 1002-1010, 2016.

Dias, F.L., Assumpção, M., Peixoto, P.S., Bianchi, M.B., Collaço, B., and Calhau, J.: Using Seismic Noise Levels to Monitor Social Isolation: An Example from Rio de Janeiro, Brazil, Geophys. Res. Lett., https://doi.org/10.1029/2020GL088748, 2020.

Díaz, J., Ruiz, M., Sánchez-Pastor, P.S., and Romero, P.: Urban seismology: On the origin of earth vibrations within a city, Scientific reports, 7(1), 1-11, 2017.

Facebook: COVID-19 Mobility Data Network. Available at: https://data.humdata.org/dataset/movement-range-maps, 2020 (accessed: 05 June 2020).

Falsaperla, S., Langer, H., and Spampinato, S.: Statistical analyses and characteristics of volcanic tremor on Stromboli volcano (Italy), Bull. Volcanol., 60(2), 75– 88, 1998.

Hong, T.-K., Lee, J., Lee, G., Lee, J., and Park, S.: Correlation between Ambient Seismic Noises and Economic Growth, Seismol. Res. Lett., XX, 1–12, doi: 10.1785/0220190369, 2020.

https://doi.org/10.5194/se-2020-136
Preprint. Discussion started: 16 September 2020

Gatto, M. et al.: Spread and dynamics of the COVID-19 epidemic in Italy: effects of emergency containment measures, Proc. Natl. Acad. Sci. USA., doi:10.1073/pnas.2004978117, 2020.

Google: COVID-19 Community Mobility Reports. Available at: https://www.google.com/covid19/mobility/, 2020 (accessed: 05 June 2020).

Graham, B.S.: Rapid COVID-19 vaccine development, Science, 368, 6494, 945-946, doi:10.1126/science.abb8923, 2020.

Hasselmann, K. A.: Statistical analysis of the generation of microseisms, Rev. Geophys., 1, 177–210, 1963.

Lecocq et al.: Global quieting of high-frequency seismic noise due to COVID-19 pandemic lockdown measures, Science, doi:10.1126/science.abd2438, 2020.

Lindsey, N. J., Yuan, S., Lellouch, A., Gualtieri, L., Lecocq, T., and Biondi, B.: City-scale dark fiber DAS measurements of infrastructure use during the COVID-19 pandemic, submitted to Science Advances.

Longuet-Higgins, M. S.: A theory of the origin of microseisms, Philos. Trans. R. Soc. London, Ser. A 243, 1–35, 1950.

Lyons, R. G.:. Understanding digital signal processing, 3/E. Pearson Education India, 2004.

Pepe, E., Bajardi, P., Gauvin, L., Privitera, F., Lake, B., Cattuto, C., and Tizzoni, M.: COVID-19 outbreak response, a dataset to assess mobility changes in Italy following national lockdown, Sci. Data 7, 230, https://doi.org/10.1038/s41597-020-00575-2, 2020.

Poli, P., Boaga, J., Molinari, I., Cascone, V., and Boschi, L.: The 2020 coronavirus lockdown and seismic monitoring of anthropic activities in Northern Italy, Sci. Rep. 10, 9404, https://doi.org/10.1038/s41598-020-66368-0, 2020.

Stein, S., and Wysession, M.: An introduction to seismology, earthquakes, and earth structure, Malden, MA, Blackwell Pub, 2003.

Trnkoczy, A.: Understanding and parameter setting of STA/LTA trigger algorithm. In: IASPEI New Manual of Seismological Observatory Practice 2 (NMSOP-2). Deutsches GeoForschungsZentrum GFZ, Potsdam, Potsdam, pp. 1–20. https://doi.org/10.2312/GFZ.NMSOP-2_IS_8.1, 2012.

Wang, D., Hu, B., Hu, C., et al.: Clinical Characteristics of 138 Hospitalized Patients With 2019 Novel Coronavirus–Infected Pneumonia in Wuhan, China, JAMA., 323(11), 1061–1069, doi:10.1001/jama.2020.1585, 2020a.

Wang, C., Li, W., Drabek, D. et al.: A human monoclonal antibody blocking SARS-CoV-2 infection, Nat. Commun. 11, 2251, https://doi.org/10.1038/s41467-020-16256-y, 2020b.

Welch, P. D.: The use of Fast Fourier Transform for the estimation of power spectra: a method based on time averaging over short, modified periodograms, IEEE Trans. Audio Electroacoust. 15, 70–73, doi:10.1109/TAU.1967.1161901, 1967.

World Health Organization, Coronavirus disease (COVID-2019) situation reports. https://www.who.int/emergencies/diseases/novel-coronavirus-2019/situation-reports/ (accessed: 21 July 2020).

Xiao, H., Eilon, Z., Ji, C. and Tanimoto, T.: COVID-19 societal response captured by seismic noise in China and Italy, Seismol. Res. Lett, XX, 1–12, doi:10.1785/0220200147, 2020.

https://doi.org/10.5194/se-2020-136
Preprint. Discussion started: 16 September 2020

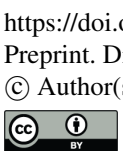

Solid Earth
Discussions
Open Access
EGU

Appendix A: additional figures

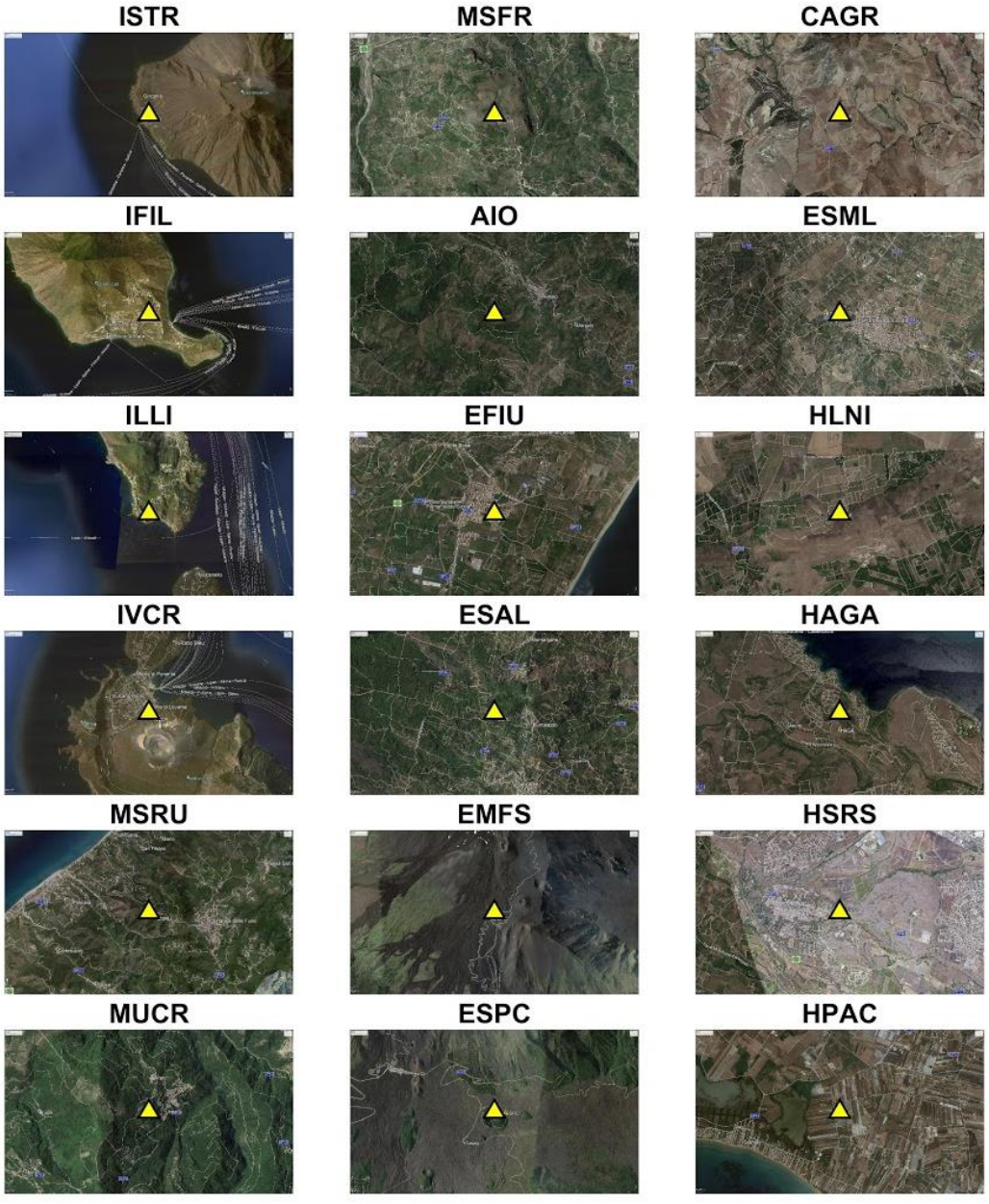

Figure A1. Photos from © Google Earth of the installation site areas of the seismic stations (yellow triangles) used in this work. The width of the area shown in each picture is ~5 km.

https://doi.org/10.5194/se-2020-136
Preprint. Discussion started: 16 September 2020

Solid Earth
Discussions
Open Access
EGU

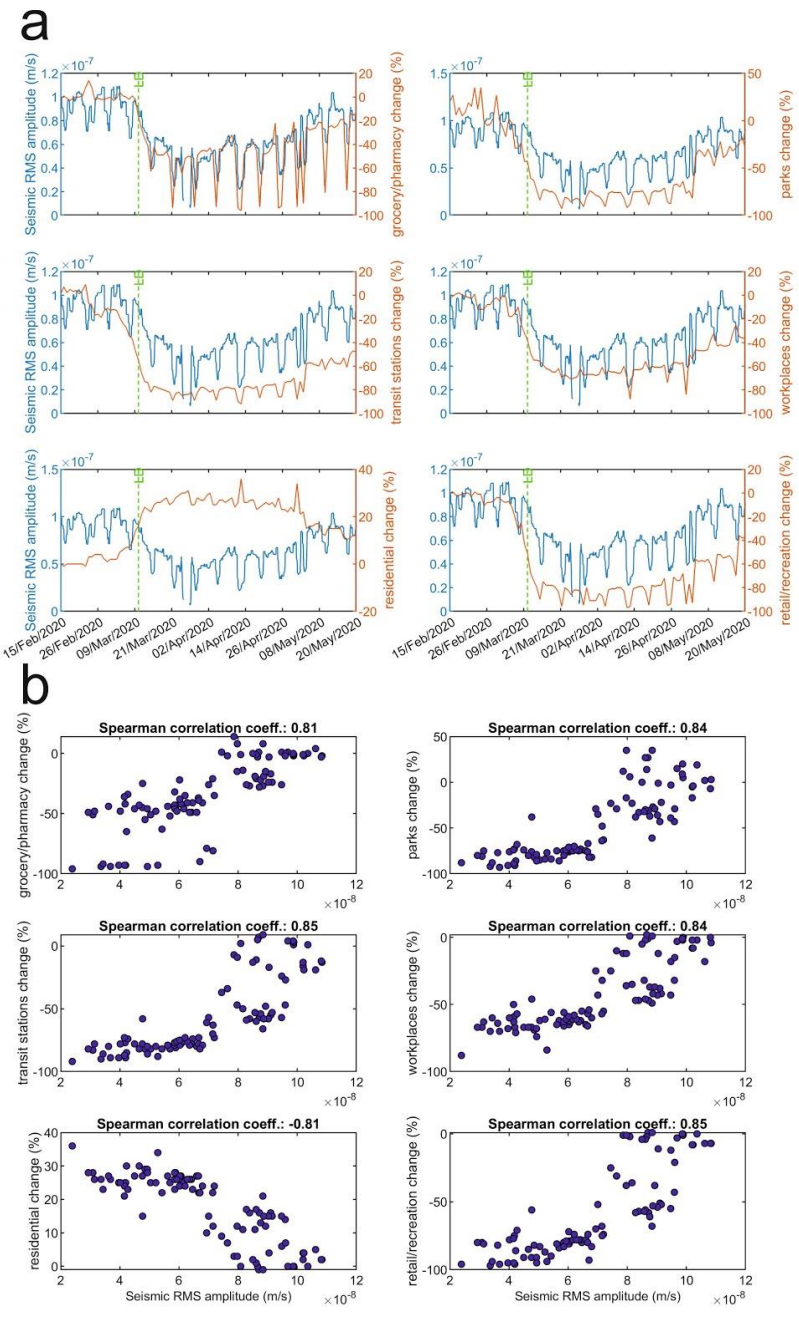

Figure A2. (a) Time series of RMS amplitude of the vertical component of the seismic signal recorded by EFIU station and filtered in the band 10-30 Hz (blue line) and of the different categories of human mobility as provided by Google (red line). The vertical dashed line and the label "LD" indicate the time when the national lockdown measures were implemented in Italy (11 March 2020). (b) Cross-plots showing the seismic RMS amplitude of EFIU station in the x-axis and the different categories of human mobility from Google in the y-axis from 15 February to 20 May 2020. The values of the Spearman correlation coefficient, computed between the time series plotted in the graph, are shown in the title.

https://doi.org/10.5194/se-2020-136
Preprint. Discussion started: 16 September 2020

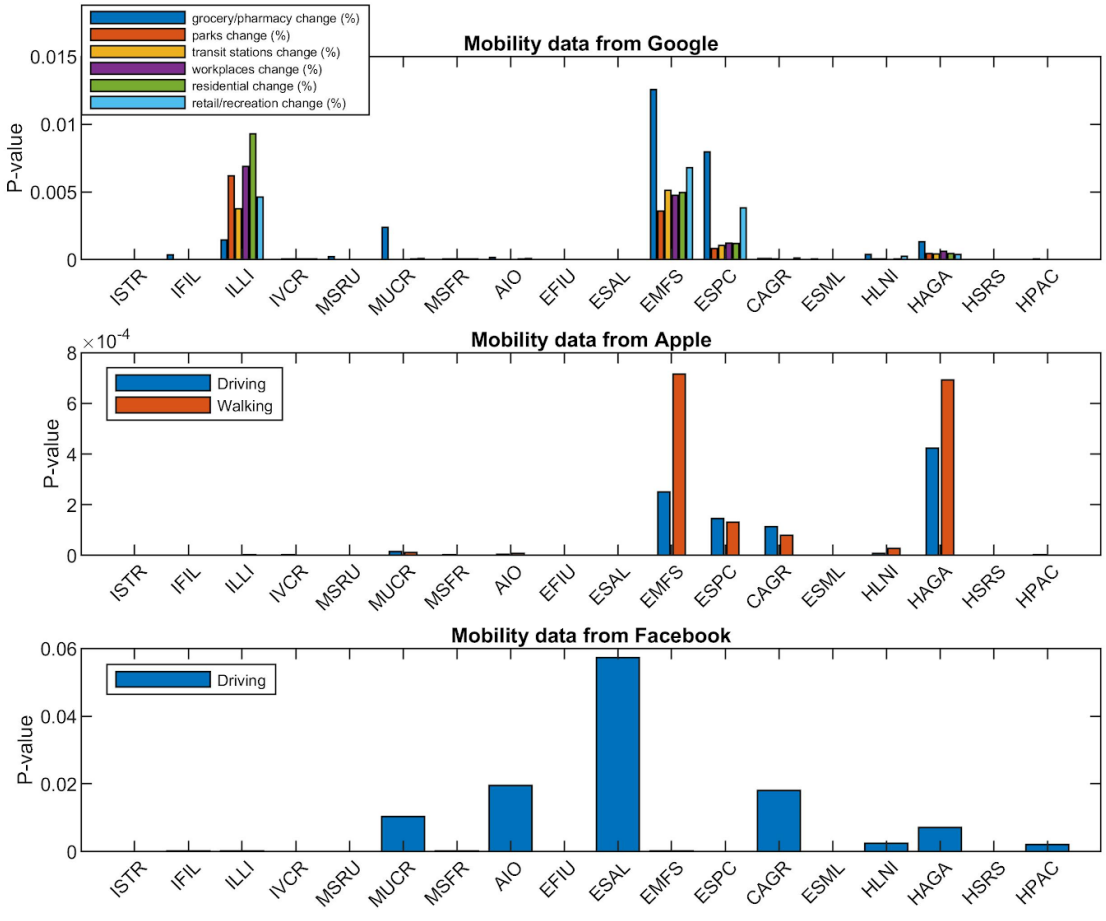

355 **Figure A3. Probability values (p-values), obtained by the Spearman correlation analysis performed between seismic RMS amplitude at the different stations and the human mobility parameters, as provided by Google, Apple and Facebook.**

https://doi.org/10.5194/se-2020-136
Preprint. Discussion started: 16 September 2020

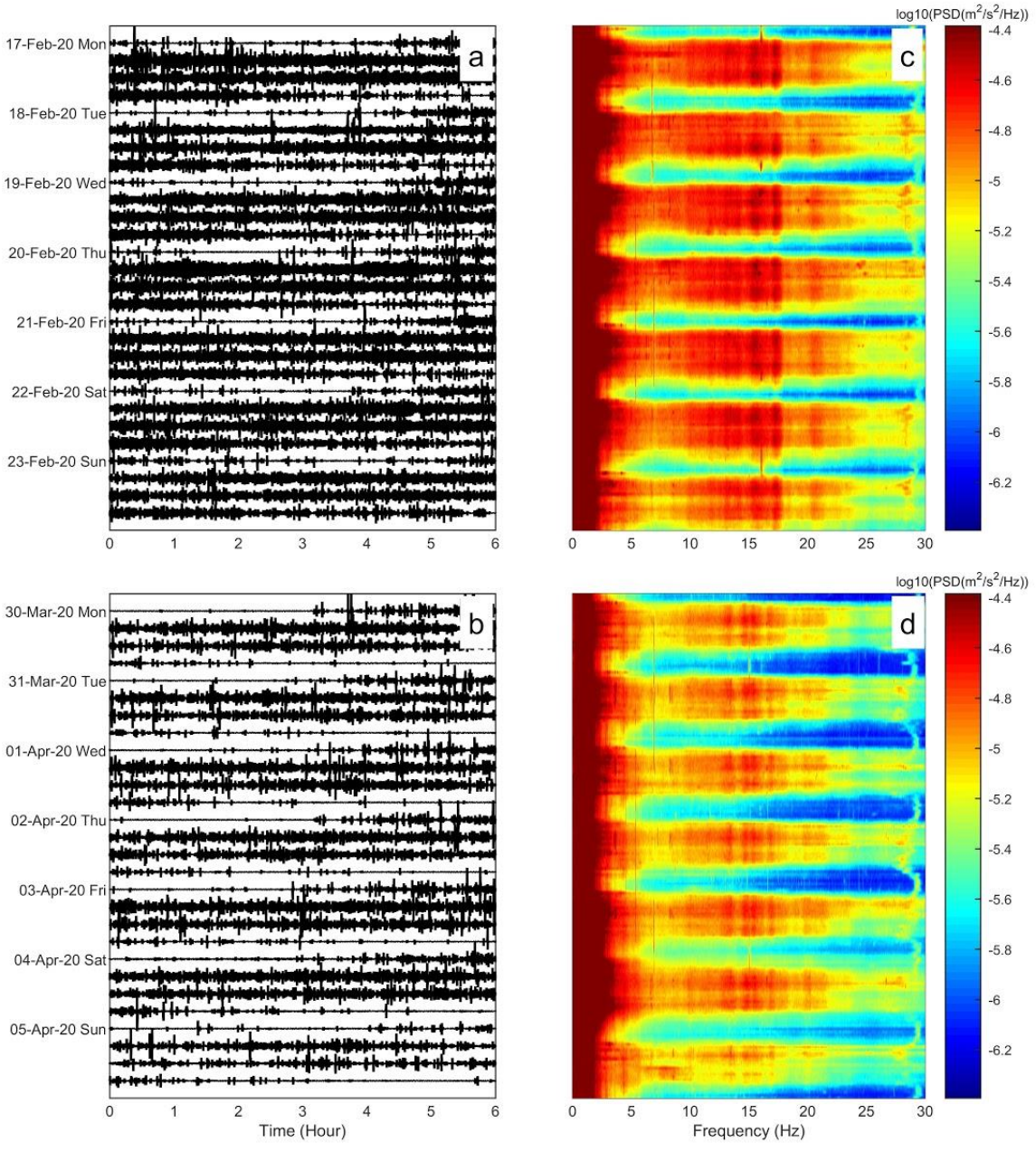

Figure A4. (a) Seismogram showing the seismic signal recorded by the vertical component of the station EFIU and filtered in the band 10-30 Hz during the week 17-23 February 2020 and (c) the corresponding spectrogram of the non-filtered signal. (b) Seismogram showing the seismic signal recorded by the vertical component of the station EFIU and filtered in the band 10-30 Hz during the week 30 March - 5 April 2020 and (d) the corresponding spectrogram of the non-filtered signal.

https://doi.org/10.5194/se-2020-136
Preprint. Discussion started: 16 September 2020

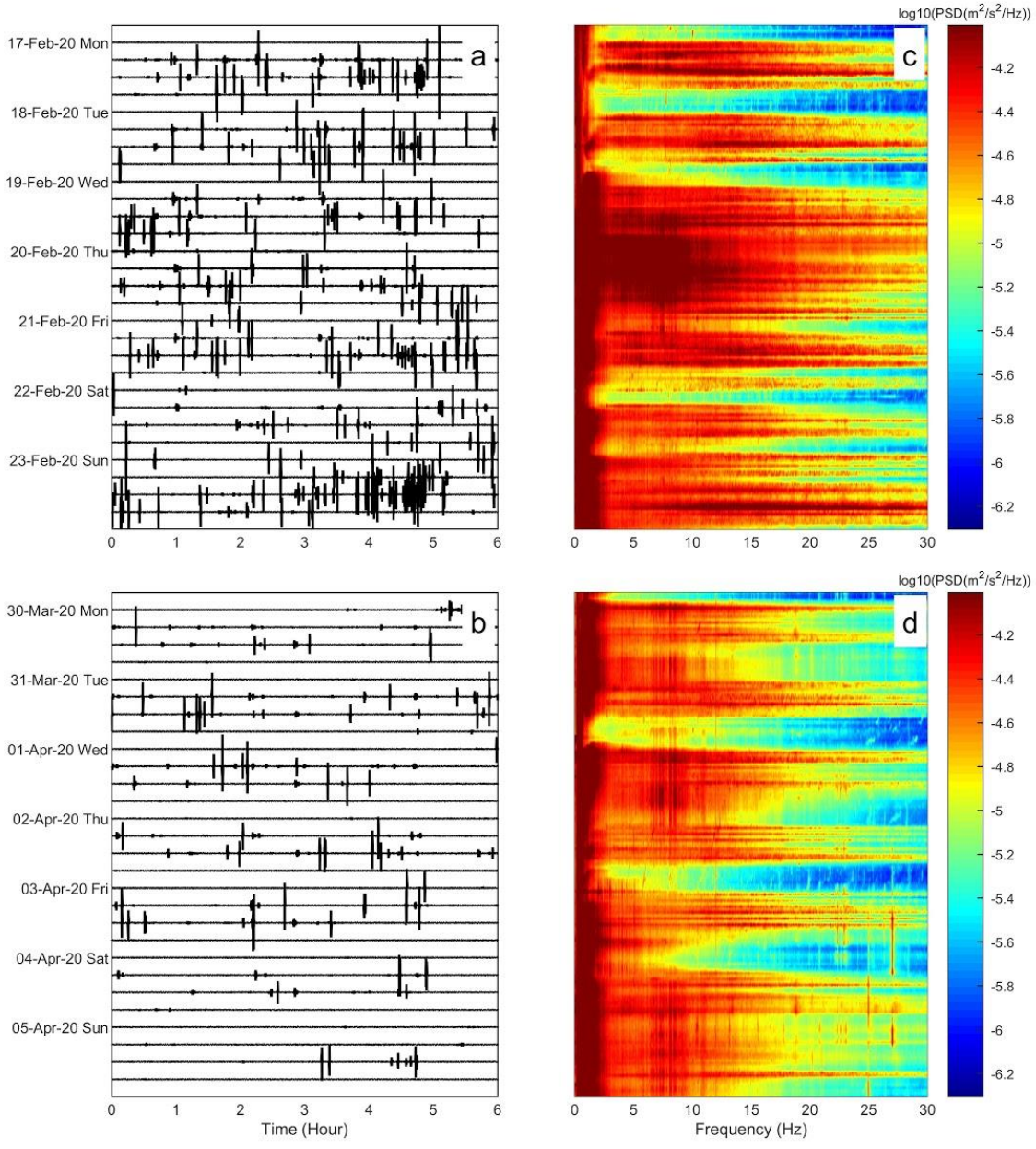

Figure A5. (a) Seismogram showing the seismic signal recorded by the vertical component of the station ILLI and filtered in the band 10-30 Hz during the week 17-23 February 2020 and (c) the corresponding spectrogram of the non-filtered signal. (b) Seismogram showing the seismic signal recorded by the vertical component of the station ILLI and filtered in the band 10-30 Hz during the week 30 March - 5 April 2020 and (d) the corresponding spectrogram of the non-filtered signal.